Surveillance of swine influenza in China during 2023-2025

Yang Huanliang

Harbin Veterinary Research Institute,
Chinese Academy of Agricultural Sciences

OFFLU SWINE INFLUENZA EXPERTS TECHNICAL MEETING
28 – 29 April 2026
WOAH Headquarters, Paris

Index

Index

Sample collection and virus isolation, 2024-2025

November, 2024- April, 2026, sample collection and testing was carried out;
28,800 nasal and tracheal swab samples from 18 provinces were collected and analyzed.

All samples were collected through abattoir-based surveillance.

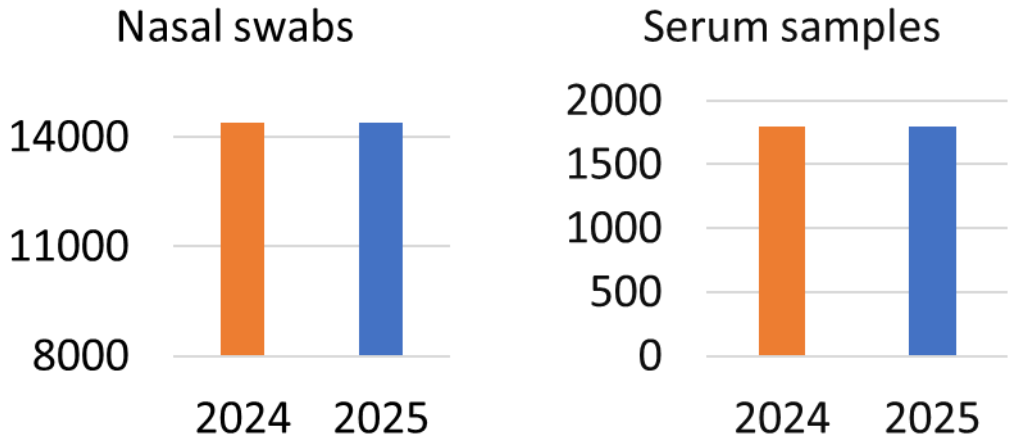

Total Nasal and Tracheal swab - 28,800
Serum samples - 3,600

Results of virus isolation

210 strains of SIVs were isolated from samples (210/14,400, 1.5%) collected in 2023.

160 strains of SIVs were isolated from samples (160/14,400, 1.1%) collected in 2024.

100+ strains of SIVs were isolated from samples collected in 2025.

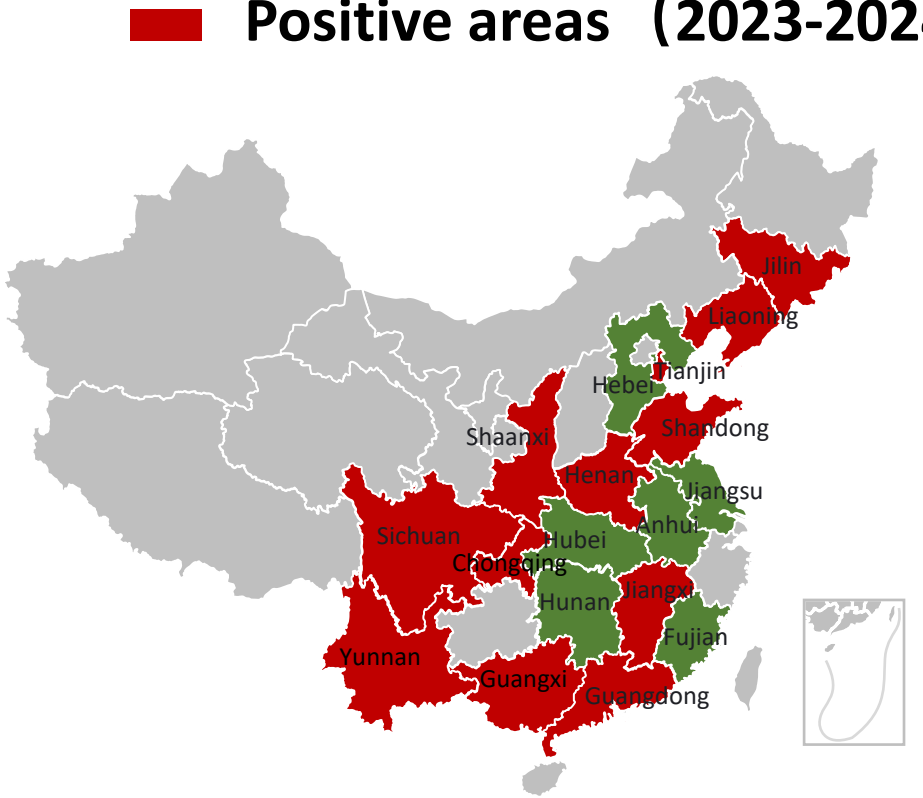

Positive areas of SI, 2023-2024
by the deadline, April, 2025

Results of virus isolation

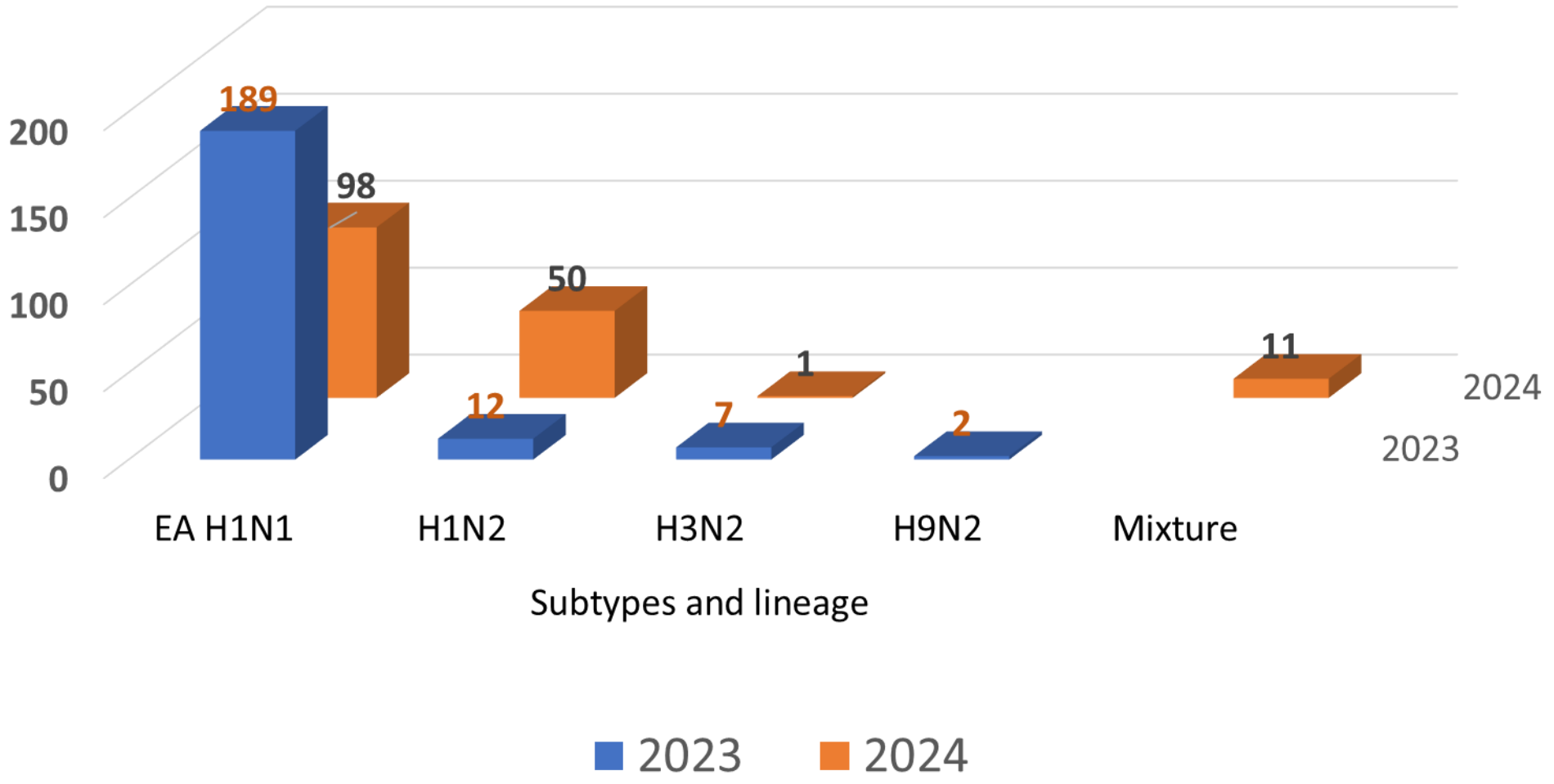

Phylogenetic tree of HA and NA genes of H1N1 subtype swine influenza virus

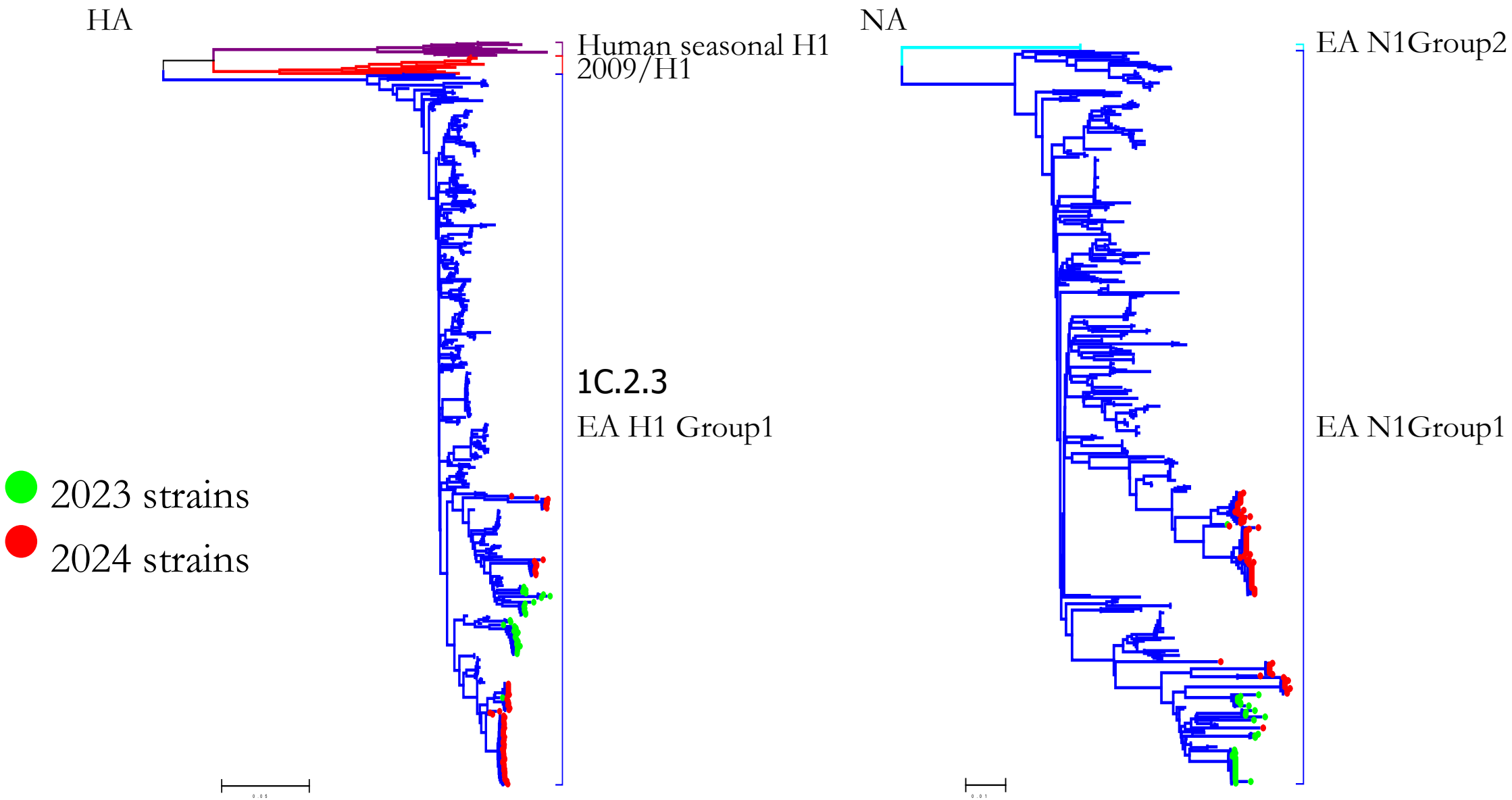

We completed whole-genome sequencing of 319 representative virus strains（2013-2019）. Based on genomic characteristics, these viruses were classified into 8 distinct genotypes (G1–G8).

Meng, F.,et al (2023). Science China-Life Sciences, 66(2), 269-282. doi:10.1007/s11427-022-2208-0

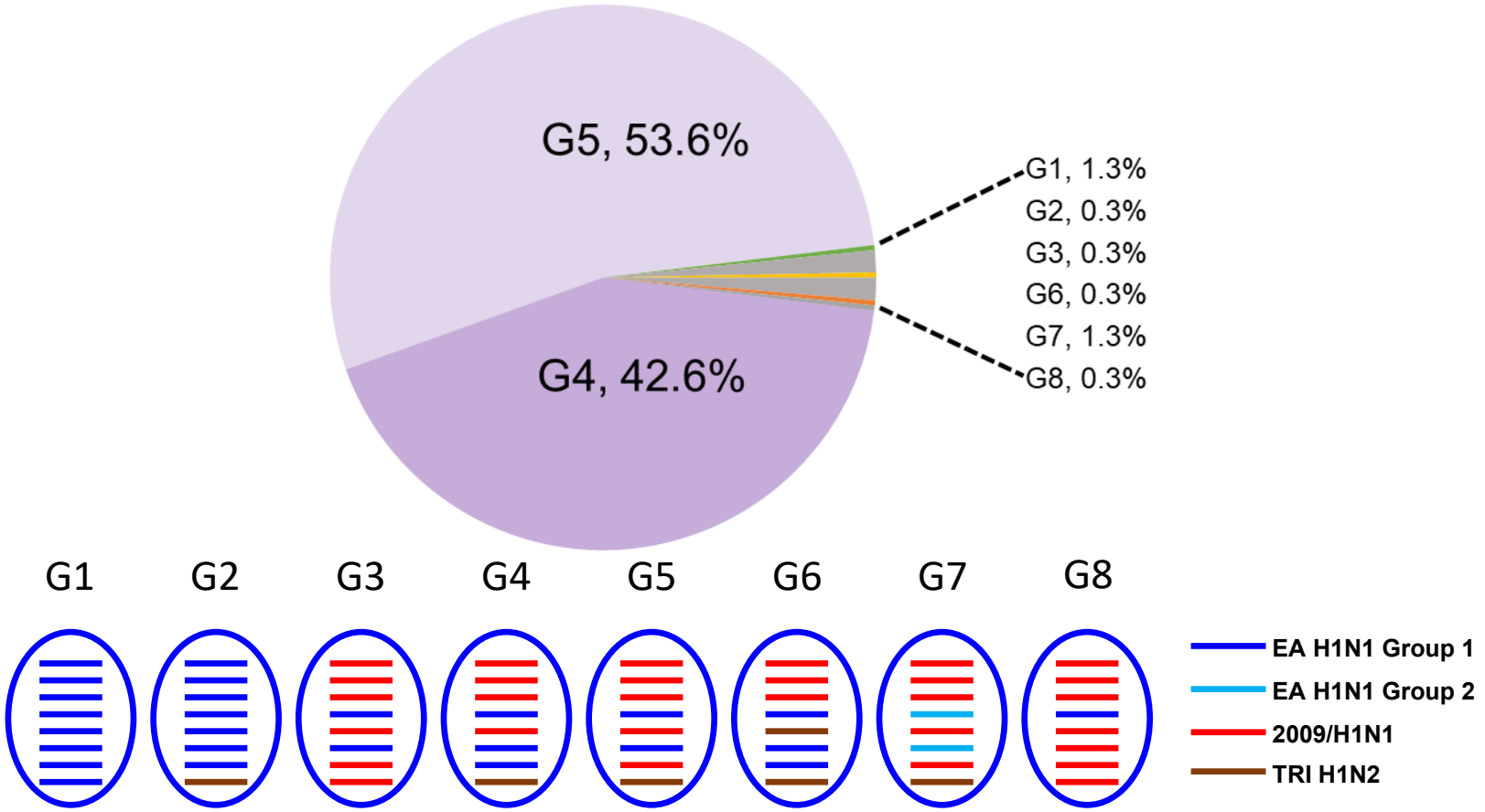

Genotypes of EA H1N1 SIVs in China (2023–2024)

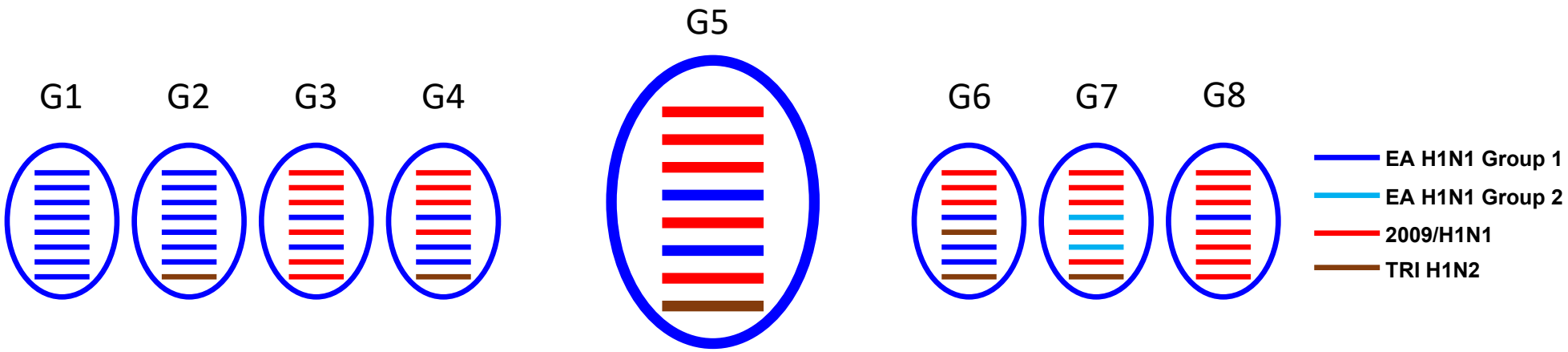

Whole-genome sequencing revealed that all EA H1N1 viruses isolated in 2023 and 2024 belonged to genotype G5.

Genotypes of H3N2 Subtype SIVs in China (2023–2024)

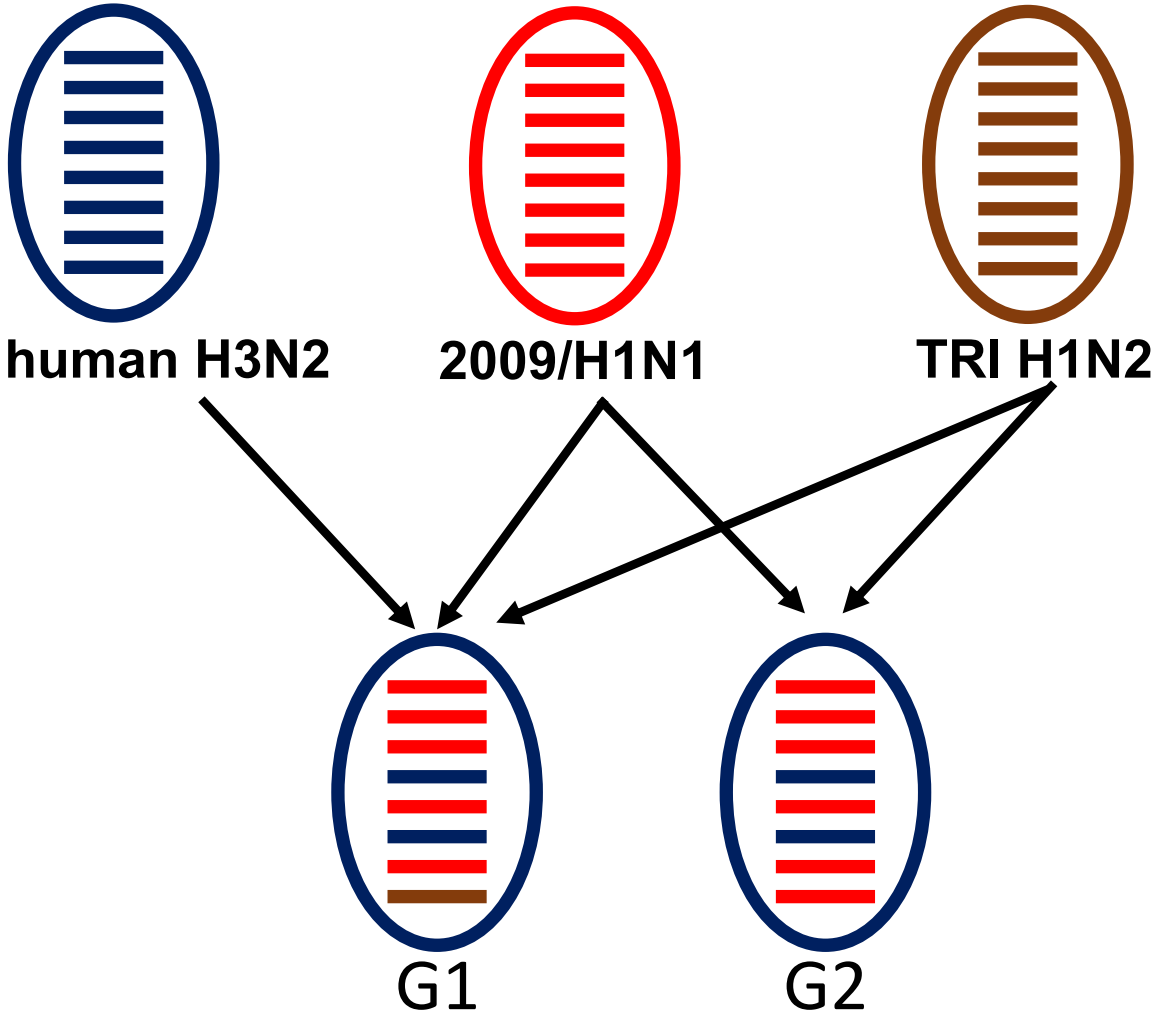

Whole-genome sequencing revealed that all H3N2 viruses isolated in 2023 and 2024 belonged to genotype G1.

HI antibodies of 1,800 serum samples, 2023

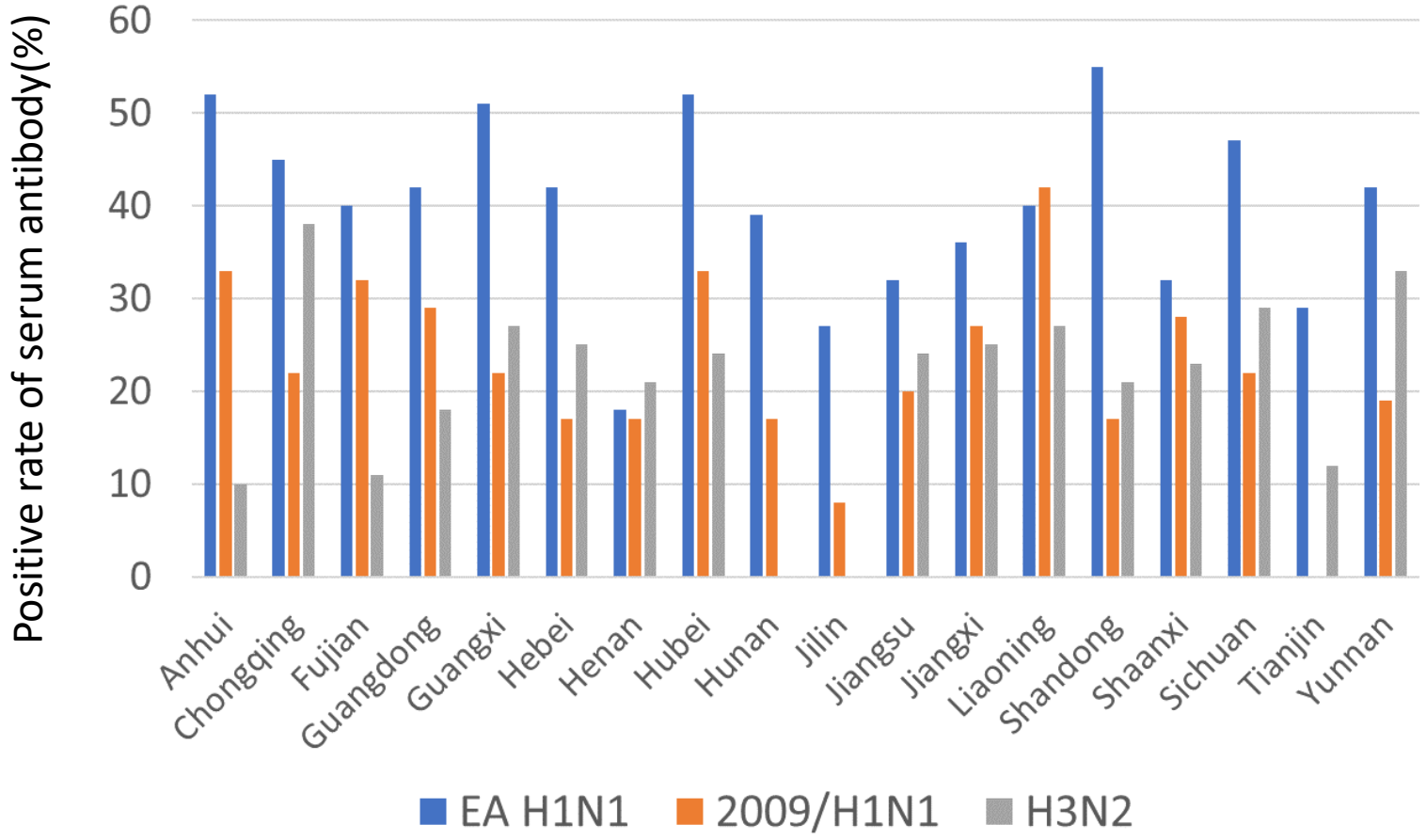

Results of HI test showed that the positive rates of EA H1N1, 2009/H1N1, and H3N2 were 40.1%, 22.5%, and 20.4%, respectively.

HI antibodies of 1,800 serum samples, 2024

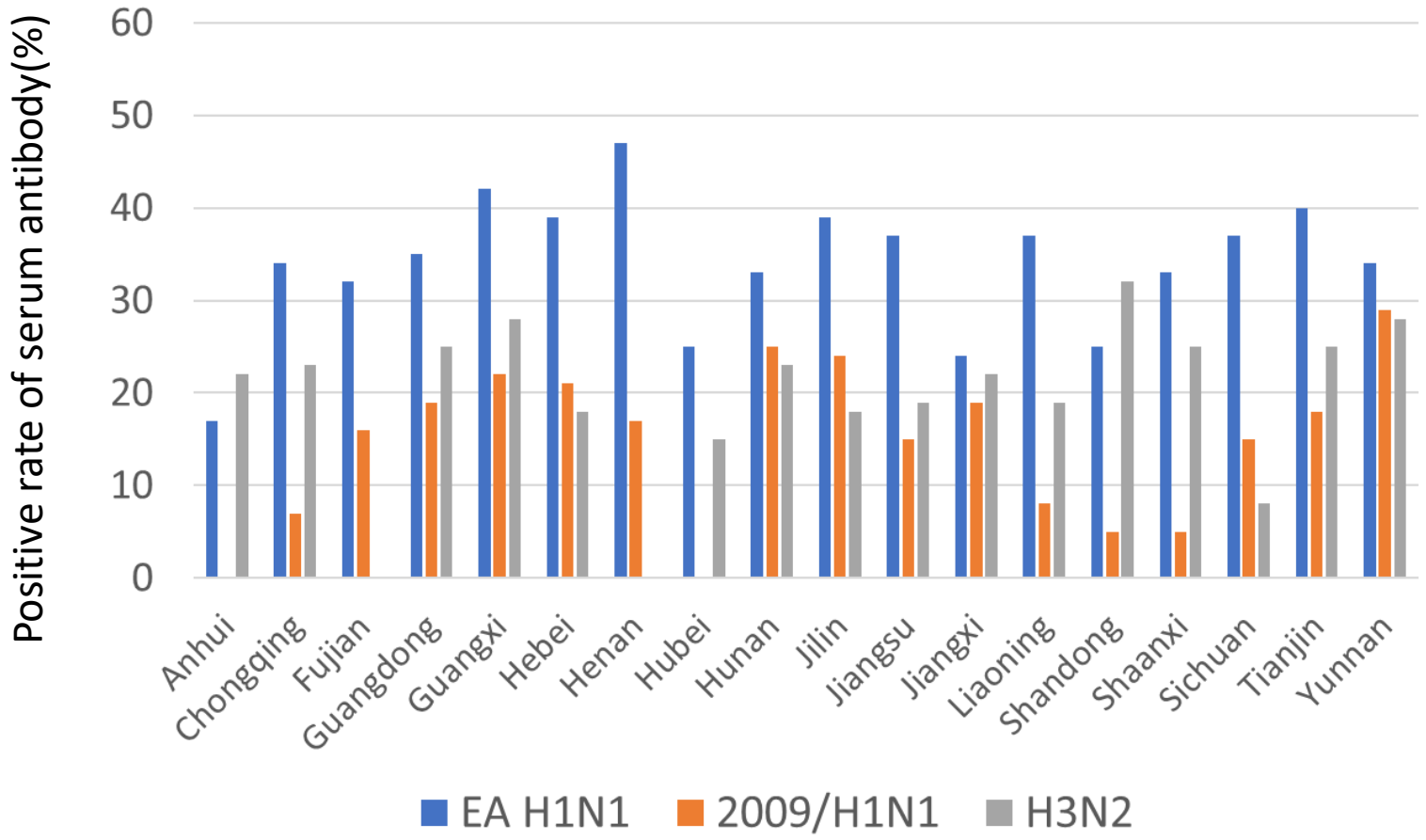

Results of HI test showed that the positive rates of EA H1N1, 2009/H1N1, and H3N2 were 33.9%, 14.7%, and 19.4%, respectively.

Index

HI titers of the H1N1 viruses with antisera of different lineage viruses

Virus	Genetic Group	Ferret Antisera			
		TJ312	GD1536	GD104	GX18
TJ312	EA1	640 [a]	80	20	640
GD1536	2009/H1N1	40	1280	20	320
GD104	EA2	<20 [b]	<20	1280	20
GX18	EA1	160	160	20	640

The HI titers of the H1N1 viruses with antisera of different lineage viruses.
Notes. [a] Homologous titers were underlined; [b] The lowest detectable level of the serum is 20.

EA H1N1 (TJ312) and 2009/H1N1 (GD1536) exhibit distinct antigenic disparities

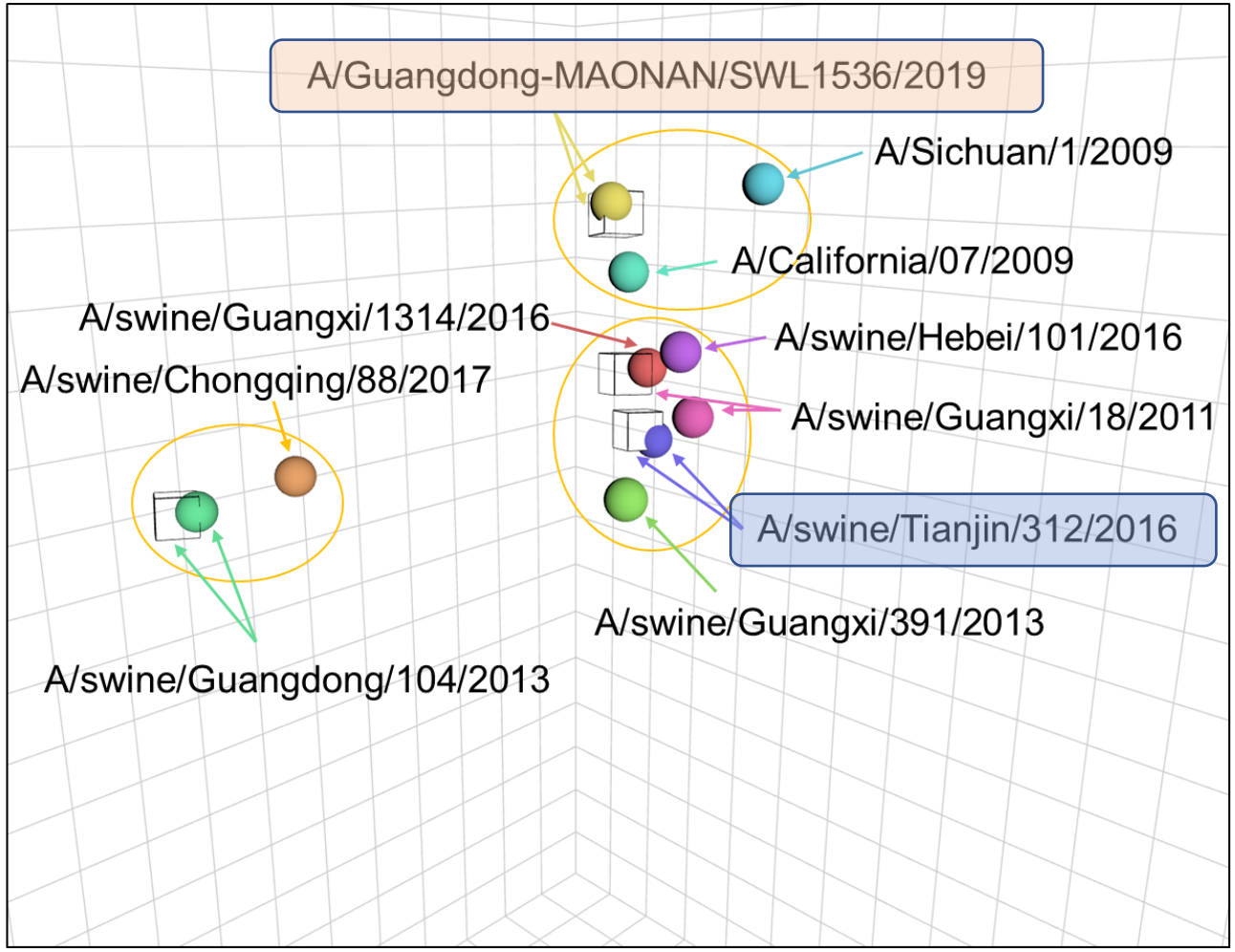

Figure. The antigenic map of the H1N1 viruses in this study. The antigenic map was created based on the HI experimental data. Squares represent the positive sera used for analysis, and circles with different color represent the viruses. The viruses within the circles belong to the same antigen group.

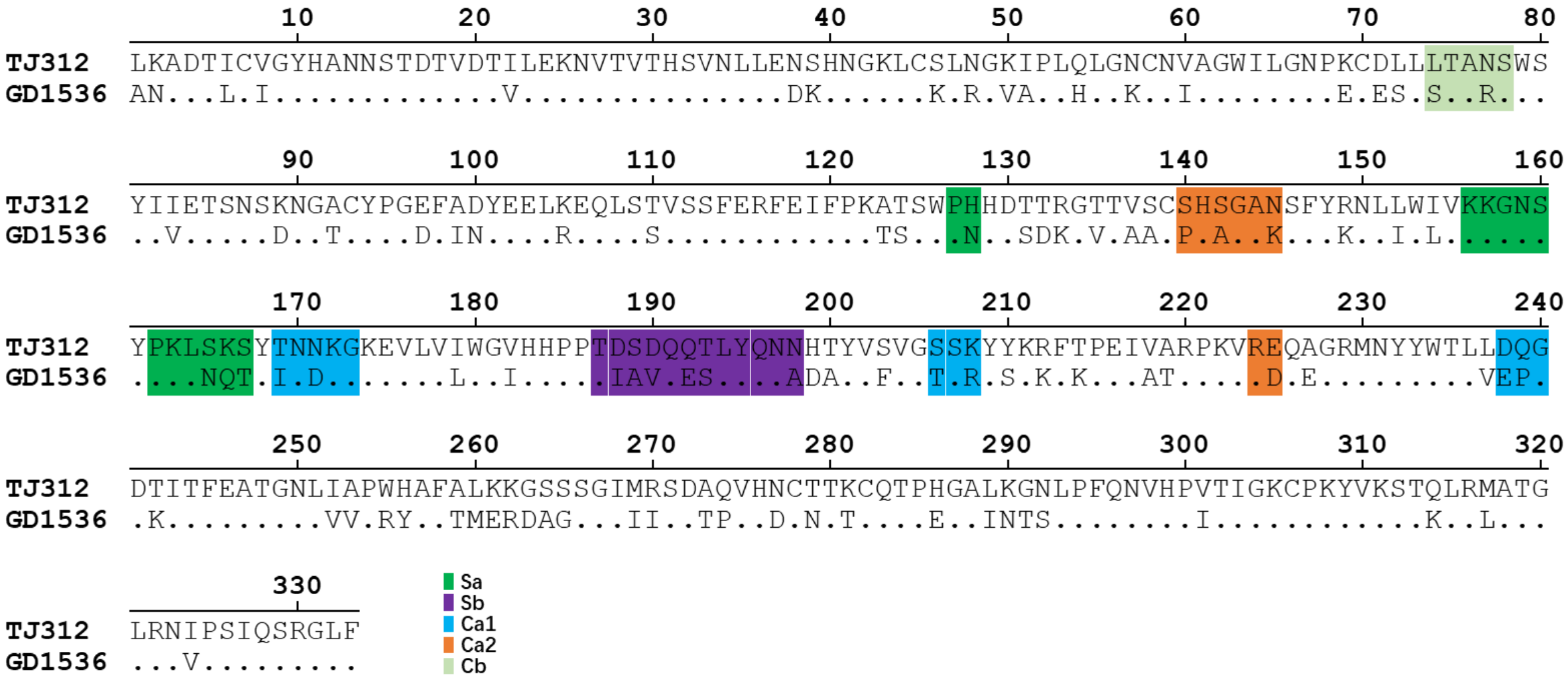

Figure. Amino acid sequence alignment of the HA1 proteins of H1N1 influenza virus strains (TJ312 and GD1536). The sequence positions are numbered according to the H3 HA numbering. Key structural features are annotated, including the receptor binding site and glycosylation sites. Sa, Sb, Ca1, Ca2, and Cb, which denote antigenic sites within the HA1 domain, are indicated in green, purple, blue, orange, and light green, respectively.

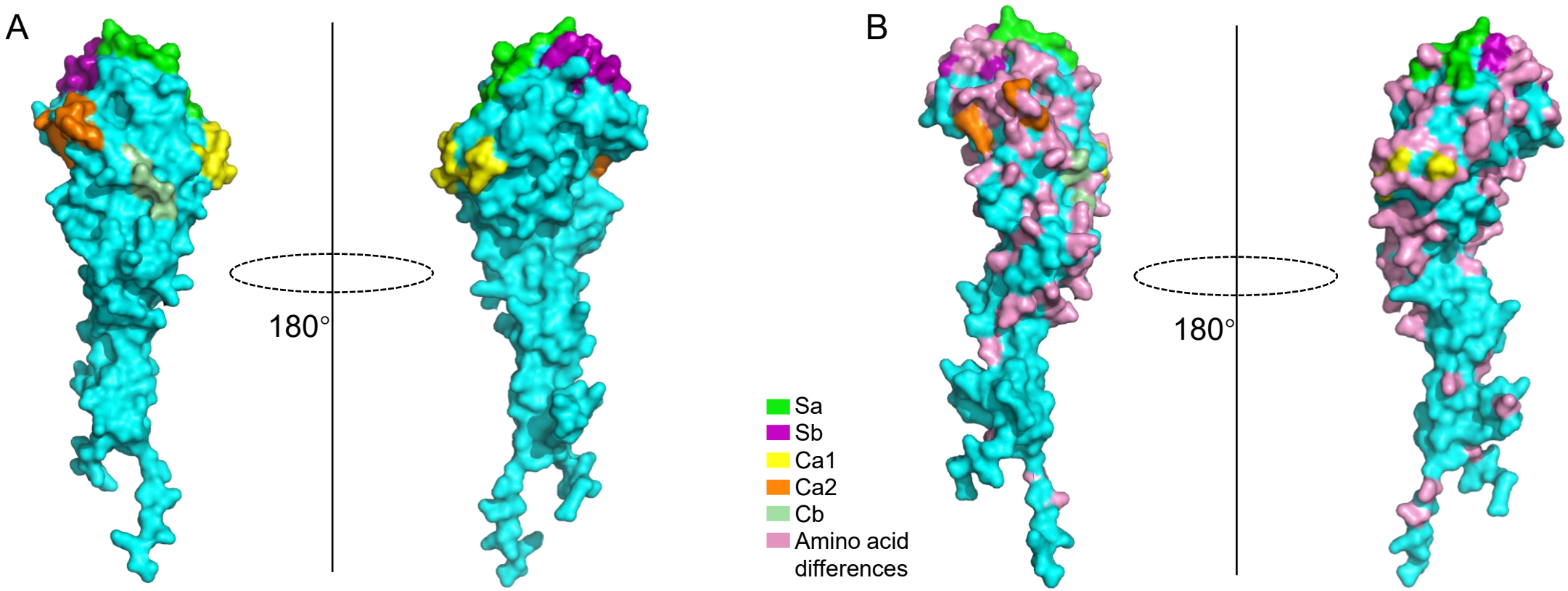

Figure. The HA1 structure of TJ312. Alphafold3 was used to predict the HA1 structure of the influenza virus TJ312, and the prediction results were visualized using Pymol software. Then, the antigenic regions of HA1 was highlighted with different colors as indicated (A), and the different amino acids between TJ312 and GD1536 in the 3D structure were marked in pink (B).

Viruses with mutations generated in the TJ312 background

Viruses	Virus Rescue	
	Mutation of HA	Successfully Rescued
TJ312/Mut-1	I6L, V8I	Yes
TJ312/Mut-2	I22V	Yes
TJ312/Mut-3	N38D, S39K	Yes
TJ312/Mut-4	S46K, N48R, K50V, I51A	Yes
TJ312/Mut-5	Q54H	Yes
TJ312/Mut-6	N57K	Yes
TJ312/Mut-7	V60I	Yes
TJ312/Mut-8	K69E, D71E, L72S, L74S, N77R	Yes
TJ312/Mut-9	I83V	Yes
TJ312/Mut-10	K89D	Yes
TJ312/Mut-11	A92T	Yes
TJ312/Mut-12	E97D, A99I, D100N	Yes
TJ312/Mut-13	K105R	Yes
TJ312/Mut-14	T110S	Yes
TJ312/Mut-15	A123T, T124S	Yes
TJ312/Mut-16	H128N	Yes
TJ312/Mut-17	T131S, T132D, R133K	Yes
TJ312/Mut-18	T135V, V137A, S138A, S140P, S142A	No [a]
TJ312/Mut-19	N145K	Yes
TJ312/Mut-20	R149K	Yes
TJ312/Mut-21	L152I, I154L	Yes
TJ312/Mut-22	S165N, K166Q, S167T, T169I, N171D	No
TJ312/Mut-23	I179L	Yes
TJ312/Mut-24	V182I	Yes
TJ312/Mut-25	D188I, S189A, D190V, Q192E, T193S	Yes
TJ312/Mut-26	N198A, H199D, T200A	Yes
TJ312/Mut-27	S203F	Yes

Viruses with mutations generated in the TJ312 background

Table 1. *Cont.*

Viruses	Virus Rescue	
	Mutation of HA	Successfully Rescued
TJ312/Mut-28	S206T, K208R, Y210S, R212K, T214K	Yes
TJ312/Mut-29	V218A, A219T	Yes
TJ312/Mut-30	E225D, A227E	Yes
TJ312/Mut-31	L237V, D237E, Q239P	Yes
TJ312/Mut-32	T242K	Yes
TJ312/Mut-33	I252V, A253V, W255R, H256Y	Yes
TJ312/Mut-34	A259T, L260M, K261E, K262R, G263D, S264A S265G	Yes
TJ312/Mut-35	M269I, R270I	Yes
TJ312/Mut-36	A273T, Q274P	Yes
TJ312/Mut-37	N277D, T279N, K281T	Yes
TJ312/Mut-38	H286E	Yes
TJ312/Mut-39	L289I, K290N, G291T, N292S	Yes
TJ312/Mut-40	V301I	Yes
TJ312/Mut-41	Q314K	Yes
TJ312/Mut-42	M317L	Yes
TJ312/Mut-43	I324V	Yes

Notes. [a] The reverse genetics system was used three times to ensure that the virus cannot be rescued.

Virus	Ferret Antisera		Virus	Ferret Antisera	
	TJ312	GD1536		TJ312	GD1536
TJ312	**640** [a]	80	TJ312/Mut-21	640	80
GD1536	40	**1280**	TJ312/Mut-22	-	-
chimeric G-T	40	1280	TJ312/Mut-23	640	40
chimeric T-G	640	80	TJ312/Mut-24	640	80
TJ312/Mut-1	640	80	TJ312/Mut-25	160	20
TJ312/Mut-2	640	40	TJ312/Mut-26	640	80
TJ312/Mut-3	640	80	TJ312/Mut-27	640	160
TJ312/Mut-4	640	80	TJ312/Mut-28	640	80
TJ312/Mut-5	640	80	TJ312/Mut-29	640	40
TJ312/Mut-6	640	80	TJ312/Mut-30	320	80
TJ312/Mut-7	640	80	TJ312/Mut-31	640	80
TJ312/Mut-8	640	80	TJ312/Mut-32	640	80
TJ312/Mut-9	640	80	TJ312/Mut-33	640	80
TJ312/Mut-10	640	80	TJ312/Mut-34	640	40
TJ312/Mut-11	640	80	TJ312/Mut-35	640	80
TJ312/Mut-12	640	80	TJ312/Mut-36	640	80
TJ312/Mut-13	640	80	TJ312/Mut-37	640	40
TJ312/Mut-14	640	80	TJ312/Mut-38	640	80
TJ312/Mut-15	640	80	TJ312/Mut-39	640	80
TJ312/Mut-16	**160**	**320**	TJ312/Mut-40	640	80
TJ312/Mut-17	320	80	TJ312/Mut-41	640	80
TJ312/Mut-18	- [b]	-	TJ312/Mut-42	640	80
TJ312/Mut-19	640	80	TJ312/Mut-43	640	80
TJ312/Mut-20	640	80	GD1536/N128H	**320**	**320**

Notes. [a] Homologous titers were marked in bold; [b] The virus was not successfully rescued; G-T is a chimeric virus composed of the HA1 of GD1536 and the HA2 of TJ312, and T-G is a chimeric virus composed of the HA1 of TJ312 and the HA2 of GD1536.

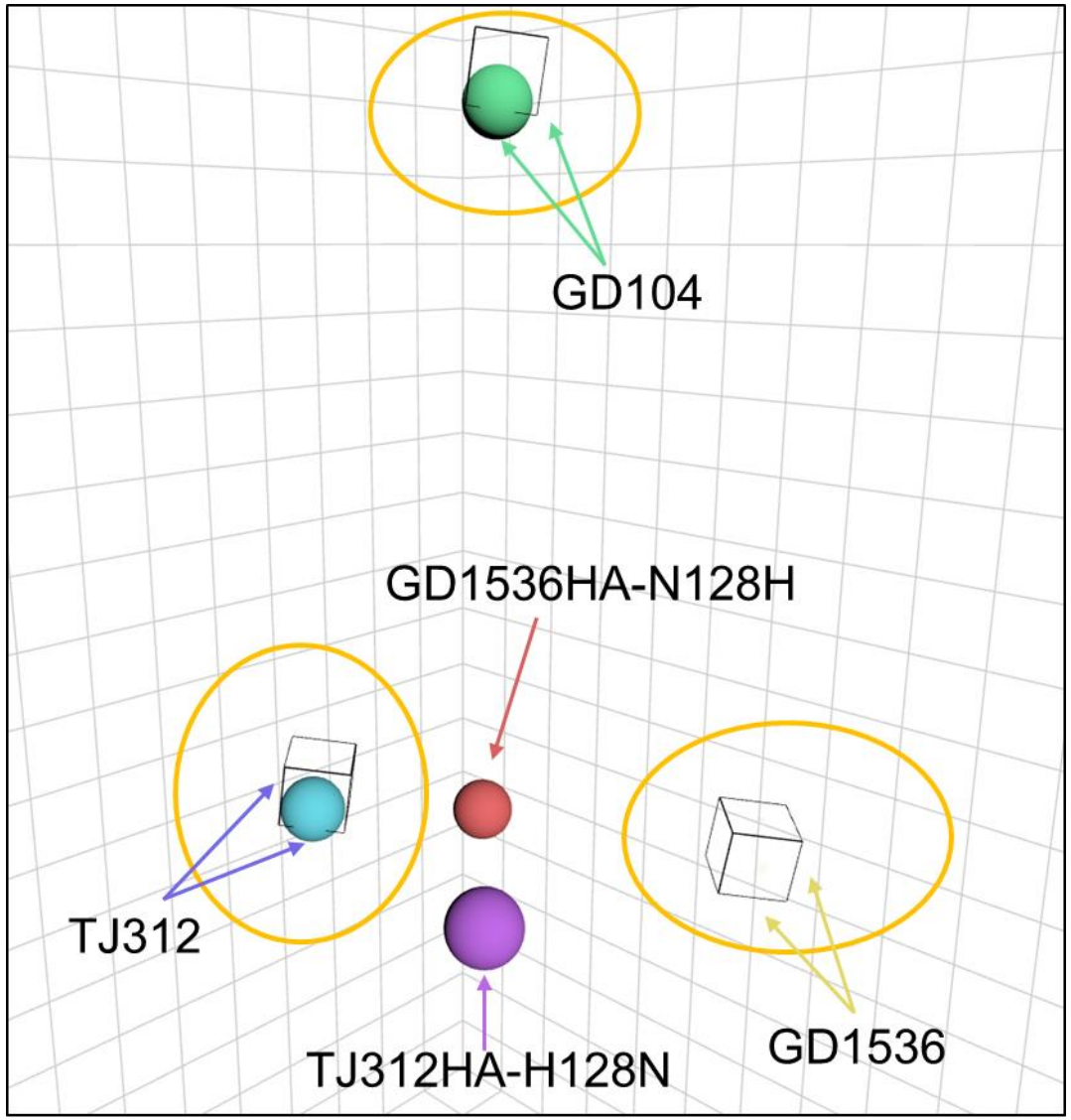

Figure. The effect of the 128N or H in HA on the antigenicity of the H1N1 strain. The antigenic map was created using the same method as in figure 1 based on the HI experimental data. In this diagram, the three yellow circles represent three antigen groups, and the mutated viruses are marked in red and purple, respectively.

Index

Figure. The 50% mouse lethal dose (MLD_{50}) of rescued reassortant viruses. Viral gene segments are denoted by colored bars. Specifically, segments originating from CQ91 and CQ445 are represented in blue and green, respectively.

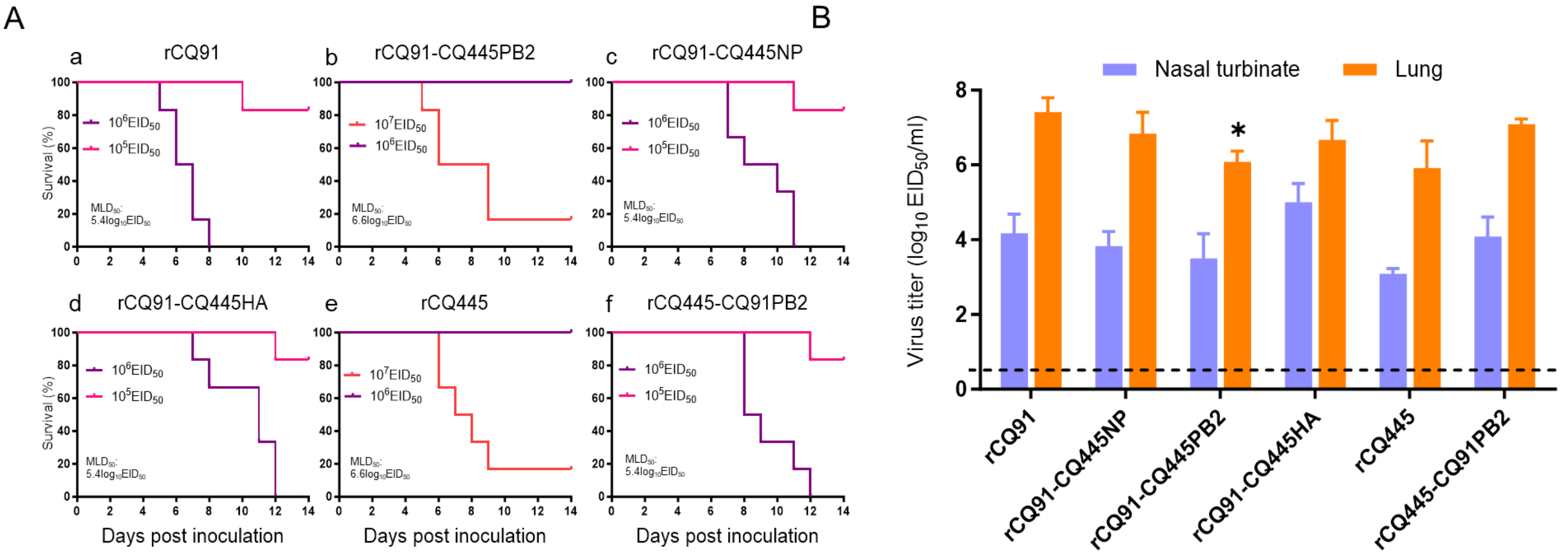

Figure. Replication and pathogenicity of rCQ91, rCQ445, and their reassortant viruses in mice. (A) Six mice per group were inoculated intranasally with the indicated doses of the six viruses and monitored for the survival rate of mice (a–f) for 14 days. Kaplan–Meier analysis and log-rank tests were used for survival estimation and group comparisons. (B) BALB/c mice were inoculated intranasally with 10^6EID_{50} of rCQ91, rCQ445, and their reassortants. Three mice per group were euthanized on day 3 post infection. Lungs and nasal turbinates were collected for virus titrations in eggs. The data shown comprise means ± SDs. * $p < 0.05$ compared with the lung virus titer values of rCQ91.

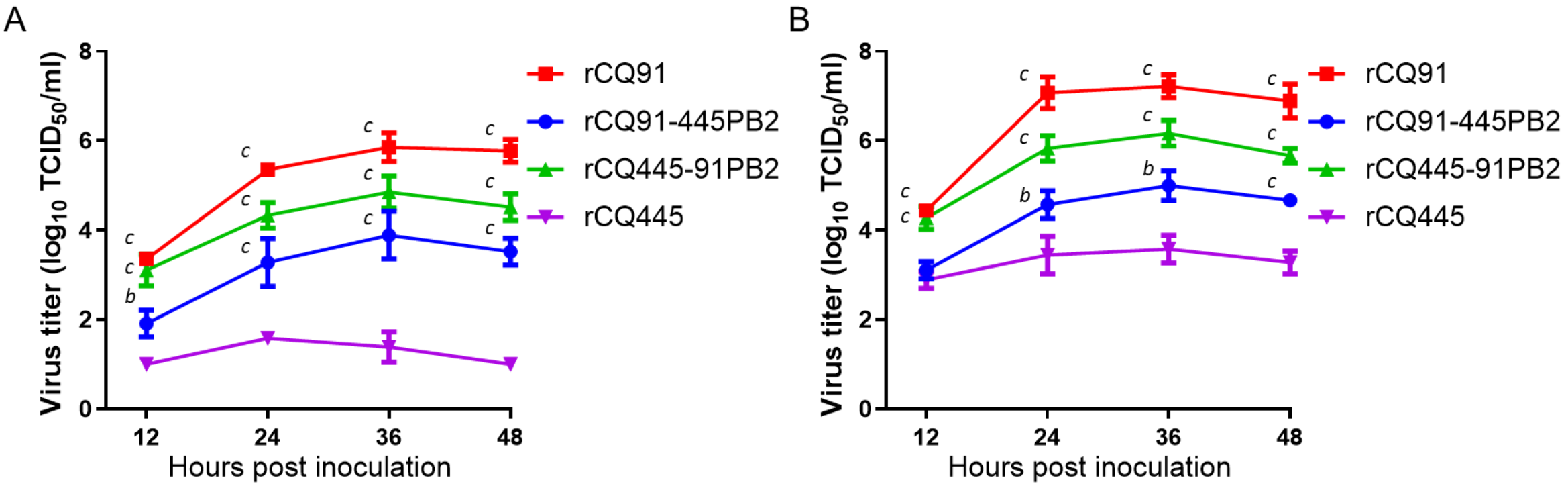

Figure. Multistep growth of rescued viruses in cultured cells. A549 (A) or MDCK (B) cells were infected with the specified viruses at a multiplicity of infection (MOI) of 0.01 and cultivated at 37°C in the presence of 1 μg/ml trypsin. Culture supernatants were collected at the designated time points, and virus titers were quantified. The data presented represent the mean ± standard deviation (SD) from three independent experiments. At each time point, data were analyzed by one-way ANOVA followed by Dennett's test by com-paring data of each group with values of rCQ445 (*b*, $p < 0.01$; *c*, $p < 0.001$).

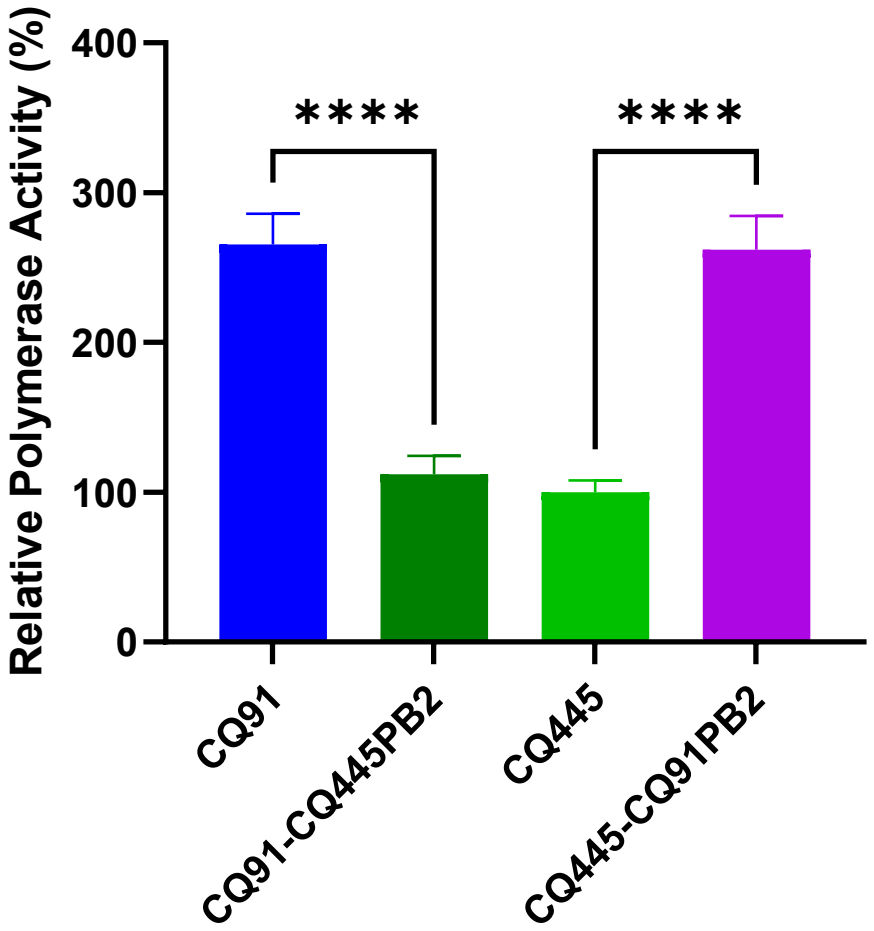

Figure. Polymerase activity of wild-type and various mutant polymerase complexes; 293T cells were transfected with plasmids expressing pCAGGS-PB1, pCAGGS-PB2 (wild-type or mutant), pCAGGS-PA, pCAGGS-NP of CQ91 or CQ445, and pPolI-NP-Luci and pRL-TK. Polymerase activity was measured at 24 hpt. All the data are presented as the means ± SDs, and comparisons were performed using one-way ANOVA. **** $p < 0.0001$ compared with the values of the vRNP of rCQ445; **** $p < 0.0001$ compared with the values of the vRNP of rCQ91. Data shown are the mean ± SD from three independent experiments.

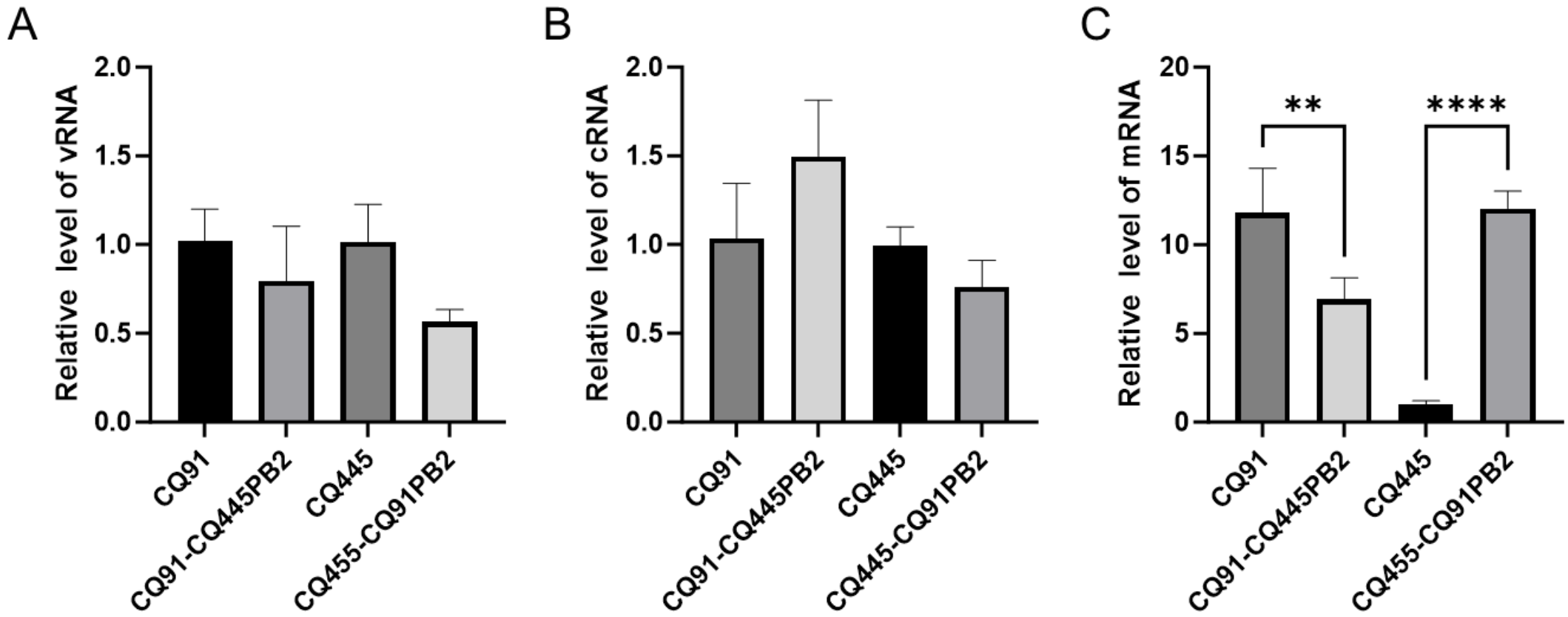

Figure. Quantitative real-time PCR results for luciferase vRNA, cRNA, and mRNA in HEK293T cells. (A–C) The pCAGGS-PB1, pCAGGS-PB2 (wild-type or mutant), pCAGGS-PA, pCAGGS-NP, and pPolI-vRNA plasmids were mixed and transfected into HEK293T cells. RNA was isolated from cells after 24 h of incubation and analyzed by a primer extension assay as described in Materials and Methods. (A) The vRNA, (B) cRNA, and (C) mRNA level of the luciferase gene. All the data are presented as the means ± SDs, and comparisons were performed using one-way ANOVA. ** $p < 0.01$, **** $p < 0.0001$. The results are from at least three different experiments.

Thank you